

Contents lists available at [ScienceDirect](http://www.sciencedirect.com)

## Journal of Herbal Medicine

journal homepage: [www.elsevier.com/locate/hermed](http://www.elsevier.com/locate/hermed)

## Research paper

# *Commiphora gileadensis* sap extract induces cell cycle-dependent death in immortalized keratinocytes and human dermoid carcinoma cells



Eitan Wineman<sup>a</sup>, Iain Douglas<sup>b</sup>, Vanessa Wineman<sup>a</sup>, Ksenia Sharova<sup>a</sup>, Marcel Jaspars<sup>b</sup>, Shiri Meshner<sup>a</sup>, Zvi Bentwich<sup>a</sup>, Guy Cohen<sup>a,\*</sup>, Avi Shtevi<sup>a</sup>

<sup>a</sup> The Skin Research Institute, The Dead-Sea & Arava Science Center (ADSSC), Ein Gedi, Israel

<sup>b</sup> Dept. of Chemistry, Marine Biodiscovery Centre, University of Aberdeen, Scotland, UK

## ARTICLE INFO

## Article history:

Received 24 March 2015

Received in revised form 28 June 2015

Accepted 31 August 2015

Available online 3 September 2015

## Keywords:

*Commiphora gileadensis*

Skin disorders

Cell cycle

Apoptosis

## ABSTRACT

*Commiphora gileadensis* is an aromatic plant traditionally used in the Middle East as a common remedy for pain and inflammation. Recently, several studies have reported on its anti-proliferative effect in cancer cell lines. Yet, scientific evidence regarding the other properties of *C. gileadensis* is limited. The aim of the current study was to investigate the cytotoxic action of *C. gileadensis* sap extracts (CgSE) on human epidermal cells and skin tissues and to ascertain its mode of action. The effects of the extract on cell viability and apoptosis were evaluated on immortalized keratinocytes, human dermal fibroblasts, human dermoid carcinoma cells and on human *ex vivo* skin cultures. CgSE significantly reduced the viability of both immortalized and transformed epidermal cells by 64% and 68%, respectively. However, normal fibroblasts and human skin organ cultures were protected from this effect. The cytotoxicity was coupled with the induction of capsase-3 and the morphological characteristics of apoptosis. In addition, CgSE-induced apoptosis did not occur in cells in the pre-replicative, G<sub>1</sub> phase, but only at later phases involved in DNA replication and cell division. HPLC analysis of CgSE showed only negligible traces of β-caryophyllene, a secondary metabolite previously isolated from *C. gileadensis* and reported to be cytotoxic. Therefore, additional active compound(s) may be involved in the anti-proliferative phenomenon of the extract. The authors concluded that CgSE contains cytotoxic products which specifically target proliferating cells in a cell cycle-dependent manner, and hence may be relevant for the treatment of skin disorders characterized by hyperproliferation, such as skin cancer and psoriasis.

© 2015 The Authors. Published by Elsevier GmbH. This is an open access article under the CC BY-NC-ND license (<http://creativecommons.org/licenses/by-nc-nd/4.0/>).

## 1. Introduction

*Commiphora gileadensis* (Cg), also known as *Commiphora opobalsamum*, is an aromatic, medium-sized evergreen shrub that grows in East Africa and Arabia. Its aromatic sap is thought to be the historical “Balm of Judea”, produced in Ein-Gedi and Jericho during the Second Temple, Roman and Byzantine eras (Hepper and Taylor, 2004; Iluz et al., 2010). Traditional Arabic medicine uses its flower and leaf decoctions both as an analgesic and to increase bowel movement and diuresis (Abdul-Ghani and Amin, 1997). In Saudi Arabia today, Cg is still considered an important medicinal plant (Al-sieni, 2014) and is used to treat swelling, pain and fever (Al-Howiriny et al., 2004b). Yet, scientific evidence regarding Cg's therapeutic properties is scarce. Al-Howiriny et al., (2004b) have reported anti-inflammatory and anti-hepatotoxic effects of orally administered Cg extract in rats. In addition, intravenous

administration of 4 mg/kg of aqueous extract of dried leaves and flowers reduced systemic arterial blood pressure and heart rate by 20% and 14%, respectively in rats (Abdul-Ghani and Amin, 1997). Recently, several new cycloartane-type triterpenoids, sesquiterpenoids and an aliphatic alcohol glycoside were isolated from ground Cg resin. Some of these compounds exhibited cytotoxic activity against human prostate, liver, and cervical cancer cell lines (Shen et al., 2007, 2008). An ethanolic Cg extract was found to inhibit growth and induce apoptosis in two lymphocytic tumor cell lines and β-caryophyllene has been identified as one of the active components in the extract (Amiel et al., 2012). A comprehensive review of *Commiphora* traditional uses, phytochemistry and pharmacology has been published recently (Shen et al., 2012).

Epidermal homeostasis involves a tight balance between proliferation and differentiation. Normally, keratinocytes that migrate from the basal layer to the skin surface, undergo terminal differentiation, and shed as cornified squames (Gandarillas and Freije, 2014). Hyperproliferative conditions, such as wound healing and the chronic inflammatory skin disease psoriasis, are associated

\* Corresponding author. Fax: +972 8 6584377.  
E-mail address: [guy@adssc.org](mailto:guy@adssc.org) (G. Cohen).

with an imbalance of these two processes (Gandarillas and Freije, 2014). Skin cancer is another hyperproliferative pathology. A typical characteristic of tumor cells that enables them to evade homeostasis is resistance to programmed cell death (Hanahan and Weinberg, 2011). Hence anticancer strategies have been devised to renew apoptosis susceptibility in tumor cells by restoring p53 activity, inhibiting the expression of anti-apoptotic Bcl-2 proteins or NF- $\kappa$ B activity, or by the induction of death receptor-dependent pathways (Chan et al., 2012; Wang and Sun, 2010).

The objective of the current study was to evaluate the anti-proliferative activity of the CgSE in several human epidermal cell models and to ascertain its mechanism of action. Specifically, the hypothesis that the extract targets proliferative cells in a cell cycle-dependent manner has been examined *in vitro* and *ex vivo*.

## 2. Materials and methods

### 2.1. Sap collection and processing

Plant matter was collected during April 2010 from a single cultivated Cg plant, grown in the medicinal plants garden of the Skin Research Institute, at Kibbutz Ein-Gedi, Israel. A voucher specimen was deposited in the herbarium of the Hebrew University of Jerusalem under reference HJ-HERB-VP-102652. Growing tips of Cg branches were cut 5 mm from the ends and flowing sap was collected immediately upon wounding, as previews described (Iluz et al., 2010). The sap was then diluted in an equal volume of ethanol, stirred for 15 min at room temperature and centrifuged (10 min, 10,000 rpm). The supernatant was designated as “*C. gileadensis* sap extract” (CgSE) and stored at  $-20^{\circ}\text{C}$ . The density of clarified CgSE was determined as  $0.883 \pm 0.023$  g/ml, by weighing a known volume of the sap following centrifugation.

### 2.2. Human cell cultures

Immortalized HaCaT keratinocytes, human dermal fibroblasts (HDF), and human dermoid carcinoma A431 were purchased from the American Type Culture Collection (ATCC). All cells were grown and maintained at  $37^{\circ}\text{C}$  in 5%  $\text{CO}_2$  in complete growth media (Dulbecco's Modified Eagle's medium; DMEM) supplemented with 10% Fetal Bovine Serum (FBS), penicillin (100 U/ml) and streptomycin (100  $\mu\text{g}/\text{ml}$ ), as previously described (Hong and Lyu, 2011; Pal et al., 2013).

### 2.3. Human skin organ culture model

Skin was obtained with informed consent from 20 to 60 years-old healthy women undergoing aesthetic abdomen reductions. All experiments were conducted with approval of the Helsinki Committee of Soroka Medical Center, Beer Sheva, Israel. Skin was cut into  $7 \times 7$  mm pieces using a mechanical press, and cultured as previously described (Portugal-Cohen et al., 2011; Portugal-Cohen et al., 2009). Briefly, the skin pieces were placed epidermal side up, in 35 mm diameter Petri dishes (Nunc, Roskilde, Denmark) containing 1 ml culture media (DMEM supplemented with penicillin (100 U/ml) and streptomycin (100  $\mu\text{g}/\text{ml}$ )) at  $37^{\circ}\text{C}$ , under 5%  $\text{CO}_2$ . To increase the sensitivity of the viability and apoptosis measurements, the epidermis was separated from the dermis as follows: the skin pieces were washed with phosphate buffered saline (PBS) and incubated at  $56^{\circ}\text{C}$  for 1 min. The epidermis was separated from the dermis with a scalpel and was allowed to recover for 1 hour prior to the measurements.

### 2.4. Viability determination by resazurin reduction assay

Cells were cultivated in 96-well plates (Nunc) in complete growth medium without or with increasing concentrations of CgSE for 24 h. After incubation, the cells were washed in PBS, and incubated with PBS containing 9  $\mu\text{g}/\text{ml}$  resazurin (Sigma, St. Louis, MO, USA) at  $37^{\circ}\text{C}$ . The fluorescent reduction product, resorufin (544 nm/590 nm), was measured using Fluoroskan Ascent Microplate spectrofluorimeter (Thermo Scientific, Vantaa, Finland). The reaction rate was measured over a 40 min period in the linear range. For the *ex vivo* skin organ cultures, the reaction rate was measured by an end-point reading at 60 min.

### 2.5. Cell death measurements

The proportion of dead cells was measured by the propidium iodide (PI) membrane integrity assay (Jones and Senft, 1985). HaCaT cells, cultivated in 96-wells plates, were incubated with 100  $\mu\text{l}$  of PI at 20  $\mu\text{g}/\text{ml}$  in PBS for 5 min at room temperature. DNA-bound fluorescence was measured at 485 nm/590 nm. Then 100  $\mu\text{l}$  of Triton X-100 solution 0.2% in double-distilled water was added to each well, and an identical second measurement was performed. Since PI does not penetrate living cells, the ratio of dead cells was deduced from the difference between DNA-bound PI fluorescence before and after cell permeabilization.

### 2.6. Apoptosis assay

Cellular apoptosis was measured using the caspase-3 activity assay (Kleszczynski et al., 2013). HaCaT, HDF, A431 or epidermis samples of equal size ( $7 \times 7$  mm) were incubated at  $37^{\circ}\text{C}$  with 100  $\mu\text{l}$  PBS supplemented with 10  $\mu\text{M}$  acetyl-DEVD-aminomethylcoumarin (Merck, Darmstadt, Germany), 0.02% Triton X-100 (Baker, Phillipsburg, NJ, U.S.A.) and 10 mM DTT. The fluorescence of released coumarin was measured at 485 nm/590 nm at 2-min intervals over a 40 min period, using Fluoroskan Ascent Microplate spectrofluorimeter.

### 2.7. Bright field, transmitted-light cell imaging

Cells were cultivated in 96-well plates and incubated with CgSE for 24 h. The cells were observed under a Zeiss Axio Observer Z1 microscope (Carl Zeiss, Jena, Germany) at 250-fold magnification. Images were acquired using Zeiss AxioCam digital camera (Carl Zeiss). For live cell imaging, the micro-culture plate was installed in a live cell chamber heated to  $37^{\circ}\text{C}$ . Bright-field transmitted light images were captured at 250-fold magnification at 5-min intervals, for a period of 24–72 h.

### 2.8. Kinetic studies of cell division and CgSE-induced apoptosis

Sub-confluent HaCaT cells were cultivated for 44 h at  $37^{\circ}\text{C}$  under 5%  $\text{CO}_2$ . The cells were then incubated with or without 1.77 w/v ppm of CgSE for 72 h. As reported previously (Orth et al., 2008), cell doubling time was determined during the first 44-h stage of the experiment and was defined as the time interval between beginning of mother cell detachment at the start of the first mitosis and the beginning of daughter cell detachment at the start of the second mitosis. Mitosis duration was defined as the time interval between the beginning of mother cell detachment and the completion of daughter cell attachment. The time interval between mitosis and apoptosis was counted from the achievement of the last cytokinesis (visual observation of cleavage furrow formation).

### 2.9. Cell cycle stage determination using Fluorescence Ubiquitination Cell Cycle Indicator (FUCCI)

A431 epidermal carcinoma cell, cultures at 50% confluence, were transiently transfected with constructs expressing the cell cycle stage markers Geminin-GFP and Cdt1-RFP under control of a ubiquitous promoter, using a commercial transfection kit (Invitrogen, Camarillo, CA, U.S.A). 16 h after transfection, the growth medium was renewed, CgSE (1.77 w/v ppm) was added, and the culture was placed on the stage of a Zeiss AxioObserver Z1 fluorescence microscope for 48 h, at 37°C under 5% CO<sub>2</sub>. Bright-field transmitted light and fluorescence images were recorded every 5 min.

### 2.10. HPLC characterization of CgSE

CgSE was analyzed by reverse phase HPLC, using a SunFire Prep C18 5 μm, 10 × 25 mm column (Waters, Milford, Massachusetts, USA) in a 1200 Infinity HPLC system (Agilent, Santa Clara, California, USA). A gradient of acetonitrile (ACN, A) in double-distilled water (B) was run as follows in a flow rate of 1 ml/min: 0–3 min, A:B (35; 65); 3–70 min, A:B (35 → 100; 65 → 0). The injection volume was 100 μl and the pressure was set at 400 bar. 5 μg of β-caryophyllene, dissolved in the mobile phase, were added to the sample as an internal standard. The elution profile was monitored by UV absorption at 230 nm.

### 2.11. Statistical analysis

Results are given as Means ± SEM. Statistical analyses were performed using Student's *t*-test. *p* < 0.05 were considered significant.

## 3. Results

### 3.1. Cytotoxic effect of *C. gileadensis* on HaCaT keratinocyte cell line

To investigate the anti-proliferative effect of CgSE, HaCaT keratinocyte cells were incubated with or without increasing concentrations of CgSE for 24 h. Fig. 1A shows a significant dose-dependent decrease in cell viability, resulting in a 60% reduction at concentrations above 1 ppm. In addition, a similar dose-dependent increase in cell death was observed when monitored by the PI membrane integrity assay (Fig. 1B). Concomitantly, caspase-3 levels were significantly augmented in CgSE-treated cells (Fig. 1C). Morphological features of apoptosis such as blebbing, nuclear fragmentation, cellular disintegration, and apoptotic bodies were also noticeable (Fig. 2).

### 3.2. Selective CgSE toxicity toward immortalized and tumor cells

We hypothesized that CgSE may have selective toxicity towards proliferating cells. Therefore, we compared the effect of the extract on epidermal carcinoma cells (A431) on immortalized but non-transformed keratinocytes (HaCaT cell line) and on normal human dermal fibroblasts (HDF). Fig. 3A shows that CgSE significantly decreased the viability of A431 carcinoma cells by 65%, in comparison with untreated control cells. This effect was slightly less pronounced in HaCaT cells (50%). Importantly, CgSE did not hamper the viability of normal dermal fibroblasts in all concentrations tested. Fig. 3B demonstrates that this toxicity was associated with increased apoptosis. Similar viability measurements were performed in normal skin organ cultures incubated for 24 h with or without increasing concentrations of CgSE. As shown in Fig. 3(C and D), CgSE did not hinder the skin viability, nor did it

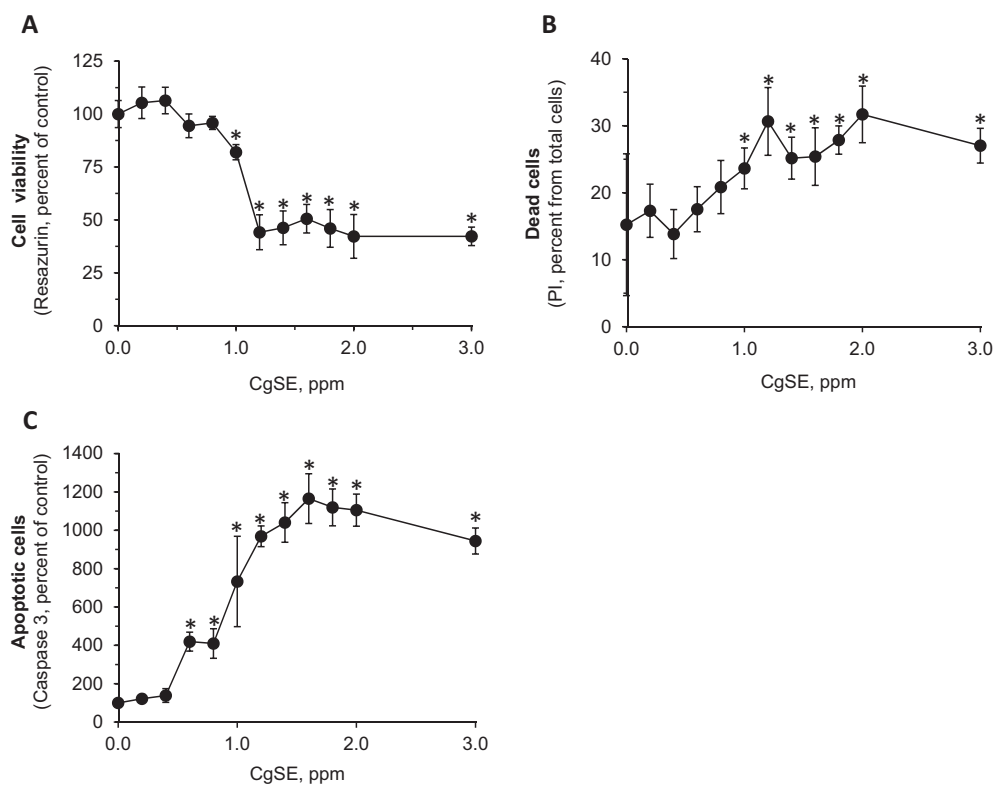


**Fig. 1.** CgSE toxicity on HaCaT keratinocytes. Cell cultures at 50% confluence were incubated with increasing CgSE concentrations for 24 h, then washed with PBS and submitted to either of the following tests. (A) Cellular viability was determined using a resazurin reduction assay. (B) Cell death was monitored by the PI membrane integrity assay. (C) Apoptosis was evaluated by caspase-3 activity, using Ac-DEVD-AMC as a fluorogenic substrate. Means ± SEM; \**p* < 0.05 for difference from the untreated control cells, *n* = 3.

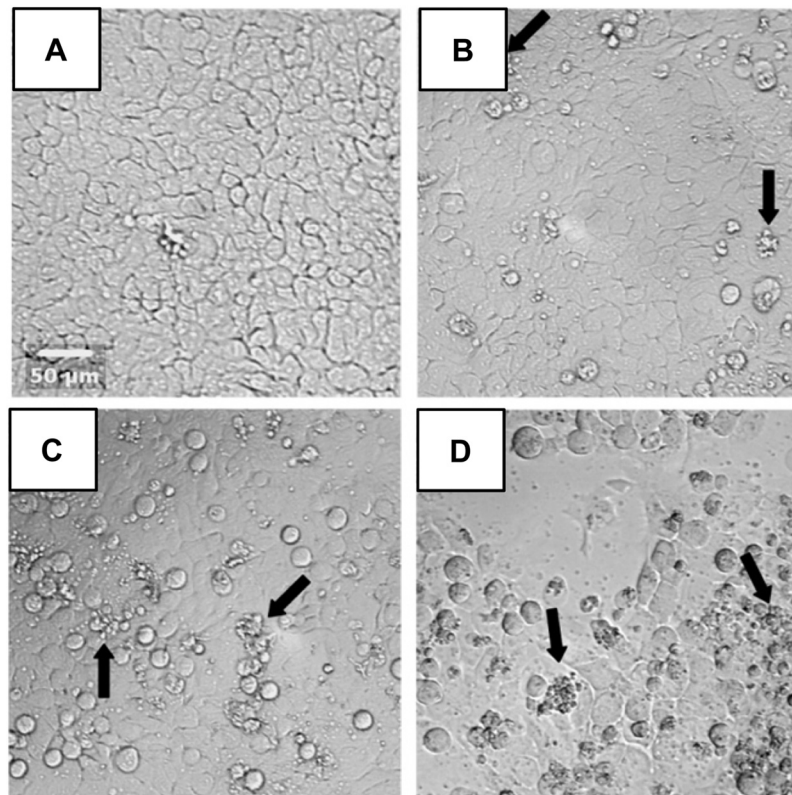


**Fig. 2.** Morphologic alterations of CgSE-treated HaCaT keratinocytes. Cells were treated as described in the legend to Fig. 1. Then, cells were observed under a phase-contrast microscope. Apoptotic features were visible from 0.6 w/v ppm and above. Arrows point to apoptotic bodies. (A) Untreated control. (B) [CgSE] = 0.6 w/v ppm. (C) [CgSE] = 1.0 w/v ppm. (D) [CgSE] = 1.2 w/v ppm. Representative images,  $n = 3$ .

induce apoptosis, in concentrations up to 265 w/v ppm in both epidermis and dermis.

### 3.3. Cell cycle dependence of CgSE-induced apoptosis, kinetic data

To investigate whether the selective toxicity of CgSE towards proliferating cells was cell-cycle dependent, live cell imaging was used to measure the average cell doubling time and duration of mitosis. Fourteen individual cells that experienced two mitotic events during the first stage of the experiment were followed. As shown in Table 1, the average doubling time was  $21:29 \pm 2:17$  h; mitosis duration was  $1:58 \pm 0:26$  h. Of note, apoptosis was observed  $22:26 \pm 4:18$  h after cytokinesis, close to the doubling time. In parallel, the average delay between CgSE exposure and apoptosis was  $11:00 \pm 5.59$  h.

### 3.4. Cell cycle dependence of CgSE-induced apoptosis, immunofluorescence data

The correlation between CgSE-induced apoptosis and the cell cycle was further analyzed by live cell imaging using the FUCCI system (Sakaue-Sawano et al., 2008). A431 epidermoid carcinoma cells were transfected with constructs expressing fluorescent Cdt-RFP (red) and Geminin-GFP (green) proteins. The nuclei of transfected cells appeared red at phase  $G_1$ , and green at phases S,  $G_2$  and M. A typical sequence of events is presented in Fig. 4, depicting two red cells in phase  $G_1$  (A and B), and two green cells in phase S,  $G_2$  or M (C and D). At the time of CgSE application (0 h), cell C appeared rounded and detached, indicating that it was approaching mitosis, while cell D was still fully attached. Six hours later, cell D also appeared rounded. After 14 h, cell C displayed the membrane blebbing (arrow) characteristic of

apoptosis, as well as nuclear cellular disintegration. During this time, the two red cells retained normal appearance and remained attached.

Table 1 depicts a set of 16 green and 12 red cells that were followed during the experiment. All green, Geminin-containing cells experienced apoptosis within 24 h. However, among the red cells that had engaged in mitosis but not yet started a new round of replication, only three apoptotic cells were detected, two of which switched to green prior to apoptosis. Thus, apoptosis took place exclusively in green cells in phases S or  $G_2$  that resulted in mitosis.

### 3.5. HPLC analysis

Several studies have linked cellular cytotoxicity of CgSE to  $\beta$ -caryophyllene, a secondary metabolite isolated from *C. gileadensis* (Amiel et al., 2012). Therefore, we performed HPLC analyses to evaluate the levels of  $\beta$ -caryophyllene in the clarified CgSE.  $\beta$ -caryophyllene levels, determined by HPLC analysis, were  $0.2 \mu\text{g}/100 \mu\text{l}$  CgSE in the undiluted crude extract (Fig. 5).

## 4. Discussion

*C. gileadensis* has been widely used for many centuries as a perfume and in traditional medicine in the Middle East (Hepper and Taylor, 2004; Iluz et al., 2010). Several therapeutic uses have been reported including anti-proliferative properties in cancer cell lines (Shen et al., 2007, 2008). The aim of the current study was to evaluate CgSE anti-proliferative effect on human epidermal cells and to ascertain its mechanism of action. Our results link CgSE cytotoxic effect to the mitotic rate in immortalized human keratinocyte cells and in A431 cells. Interestingly, normal fibroblasts and human *ex vivo* skin cultures were protected from



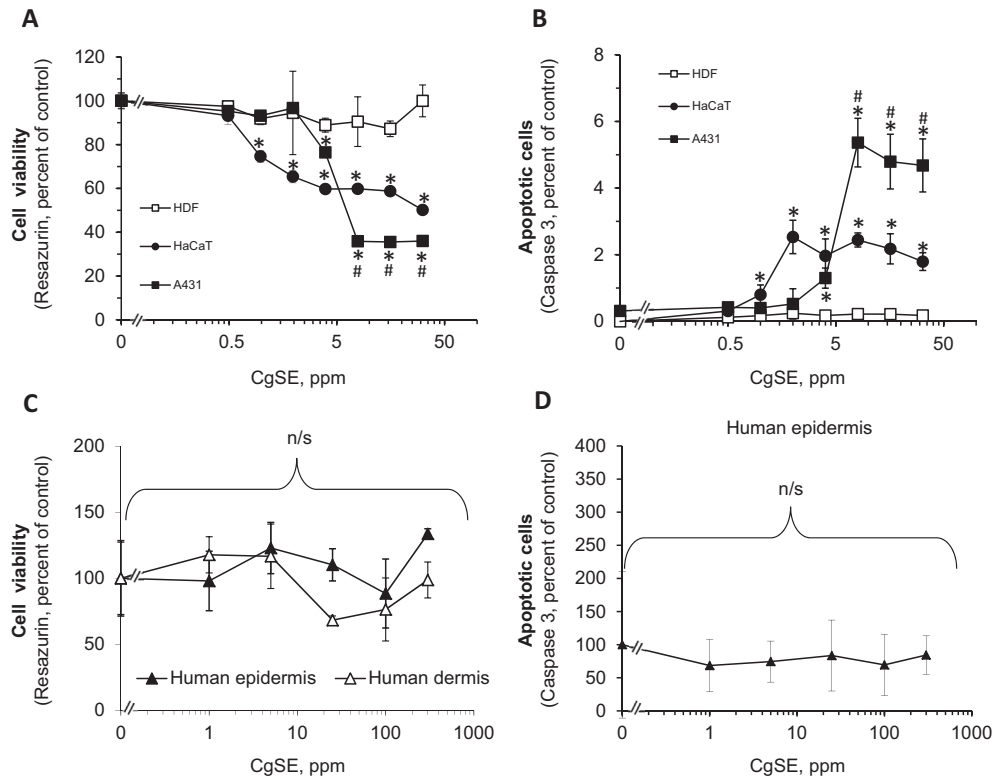


**Fig. 3.** Selective toxicity towards immortalized and tumor cells. Cultures of normal dermal fibroblasts (HDF), spontaneously immortalized keratinocytes (HaCaT) and epidermal carcinoma cells (A431) were incubated with CgSE, then cellular viability was determined by the resazurin assay (A) and apoptosis by caspase 3 assay (B). (C) Organ cultures were incubated for 24 h with increasing CgSE concentrations, and then dermis and epidermis were separated and submitted separately to the resazurin assay. (D) Organ cultures were processed similarly, with the epidermis assayed for caspase-3 activity. Means  $\pm$  SEM; \* $p < 0.05$  for difference from the untreated control cells; # $p < 0.05$  for difference from the untreated control cells,  $n = 3$ .

**Table 1**

Kinetic correlation between HaCaT cell division and CgSE-induced apoptosis.

	Doubling time	Mitosis duration	Time interval from CgSE exposure to apoptosis onset	Time interval from last cytokinesis to apoptosis onset
Average	21:29 $\pm$ 2:17 h	1:58 $\pm$ 0:26 h	11:00 $\pm$ 5:59 h	22:26 $\pm$ 4:18 h
No. of cells	27	15	14	14

CgSE-induced apoptosis correlates with A431 cell cycle: Cells were treated as described in the legend to Fig. 4. The table summarizes the doubling time, mitosis duration and the time interval recorded over a period of 24 h.

the toxic action of the extract. Importantly, the current data suggest that the cellular toxicity observed in the immortalized keratinocytes and in the human dermoid carcinoma cells was dependent on the cell cycle phase of the cells.

Exposure of immortalized keratinocyte cell line and of A431 dermoid carcinoma cells to CgSE resulted in the induction of apoptosis and their subsequent death, evident from the typical morphological changes observed in programmed cell death and the increase in caspase 3 activity. It should be noted that higher concentrations of CgSE were required for toxicity to appear in A431 than in HaCaT cultures, displaying dose-dependence from 1.77 to 7.06 w/v ppm and from 0.35 to 1.06 w/v ppm, respectively. The difference may be due to cell type variance or to the inherent protection of carcinoma cells from apoptosis. Importantly, both human fibroblasts and the human *ex vivo* skin organ culture could tolerate CgSE at much higher concentrations (28 and 265 w/v ppm, respectively). These results demonstrate that CgSE exerts selective cytotoxic effects on immortalized and transformed skin cells. Of note is that Cg extracts, administered to rats intravenously up to 4 mg/kg, or orally up to 500 mg/kg, were well tolerated and non-

toxic (Abdul-Ghani and Amin, 1997; Al-Howiriny et al., 2004a), indicating its safety and potential therapeutic window.

To demonstrate the cell cycle specific toxicity of the CgSE, the Fluorescent Ubiquitination-based Cell Cycle Indicator (FUCCI) system was used. Two fluorescent cell cycle markers, Geminin-GFP and Cdt1-RFP were co-transfected to the cells. In the replication cycle, the replication origins need to be "licensed" by the Cdt1 factor. This crucial event is restricted to the post-mitotic G1 phase. Geminin is a positive regulator of DNA replication and inhibits Cdt1 activity. It is absent during G0/1 phases, and accumulates through S, G2 and M phases (Caillat and Perrakis, 2012). Thus, by monitoring the interchange between these two factors, the cytotoxic effect on specific cell cycle phase can be measured. Using both FUCCI and live cell imaging in bright-field, it was shown that CgSE-induced apoptosis correlated with mitosis, since cells did not divide after CgSE exposure, but died by apoptosis at the expected time of cell division. In addition, cells in the post-mitotic, pre-replication G1 phase well tolerated CgSE treatment. In contrast, CgSE induced apoptosis in cells already engaged in the process of DNA replication and committed to mitosis. Indeed,

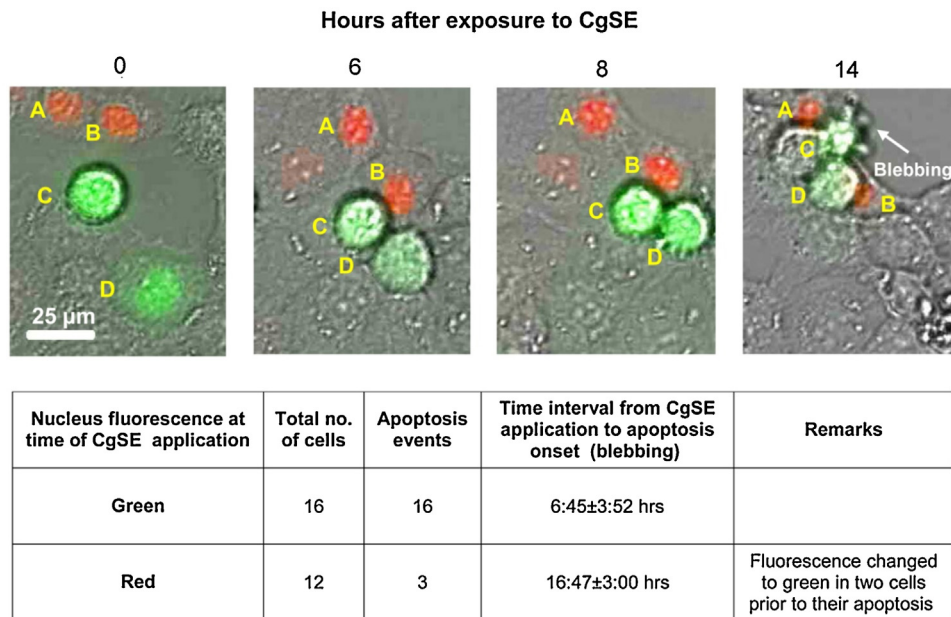


**Fig. 4.** Correlation between A431 cell cycle and CgSE-induced apoptosis. A431 epidermal carcinoma cells were transfected to express the cell cycle markers Geminin-GFP (stages S, G<sub>2</sub> and M, green fluorescence) and Cdt1-RFP (stage G<sub>1</sub>, red fluorescence), and then exposed to CgSE (1.77 w/v ppm). 16 green cells and 12 red cells were followed in live imaging. A sequence of images shows the fate of a group of two red cells (A and B) and two green cells (C and D) as a representative example. The red cells showed no sign of apoptosis, while the two green cells appeared first to detach, an early sign of either mitosis or apoptosis, and finally to bleb, a characteristic feature of programmed cell death, visible in cell C at 14 h (arrow). [Table 1](#) summarizes the observations made on the whole group of cells over a period of 24 h. (For interpretation of the references to color in this figure legend, the reader is referred to the web version of this article.)

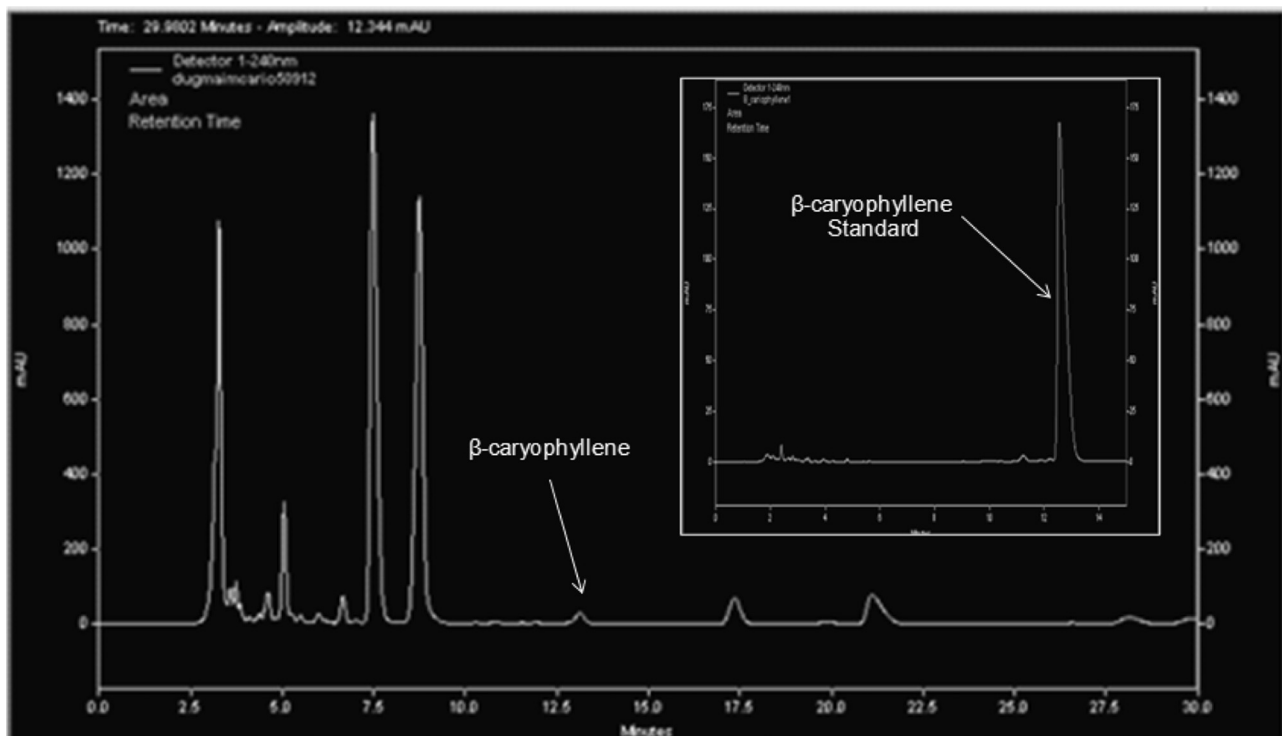


**Fig. 5.** CgSE HPLC profile. 100 µl of CgSE, diluted 1:10 in acetonitrile were loaded on a reverse phase chromatography column and eluted as described in Materials and Methods. Insert: HPLC analyses of β-caryophyllene standard (5 µg) that shows a peak after 14 min. Representative images,  $n = 3$ .

mitosis never occurred after CgSE treatment, confirming that the cell cycle was affected. Importantly, apoptosis took place exclusively in the S or G<sub>2</sub>, phases, indicating that CgSE toxicity was cell cycle specific and targeted only mitotic cells.

The reported cytotoxicity of Cg extracts in prostate cancer cells (Shen et al., 2013, 2007) and their reported anti-inflammatory properties (Al-Howiriny et al., 2004b) can be interpreted as a lethal effect directed at proliferating tumor cells and suppressive effect

on cells of the immune system, respectively. Recently, Cg extracts were shown to induce cell death in mouse and human transformed lymphocytes, with evidence for DNA degradation that is a characteristic of apoptosis (Shen et al., 2012). The results of our study suggest that the mechanism of action of Cg toxicity towards tumor cells is due to their fast replication time and the subsequent increase in the mitotic phase.

The effect of CgSE on stem cells in epithelial tissue had not been investigated so far. It can be speculated that stem cells undergoing frequent mitotic events for the purpose of skin renewal or regeneration would be equally affected by the cytotoxic effects of CgSE. However, this would require the active compound(s) from the CgSE extract to penetrate the tissue in order to reach the stem cells located in the basal layer (stratum basale). The results obtained using the *ex vivo* human skin cultures indicate that the stem cells in epithelial tissue are protected, suggesting low permeation of CgSE through the external layers of the epidermis. Further work should be conducted to assess the permeability, safety and therapeutic window of topically administered CgSE.

*Commiphora mukul*, a plant species related to Cg produces a sterol, guggulsterone that inhibits proliferation in a number of human tumor cell lines through inhibition of DNA synthesis and cell cycle arrest in the S phase (Agrawal et al., 2004). Guggulsterone induces apoptosis by activation of c-Jun N-terminal kinases (JNK), suppression of Akt pathway and downregulation of anti-apoptotic functions (Shishodia et al., 2007). Cg could be a source of guggulsterone-like molecules with similar properties. Amiel et al. (Amiel et al., 2012) raised the hypothesis that Cg cytotoxicity may be associated with  $\beta$ -caryophyllene, a compound present in Cg stem extracts, the oxide of which is known to inhibit growth and to induce apoptosis in human cancer cells. Therefore we hypothesized that  $\beta$ -caryophyllene has a key role in the cell cycle specific cytotoxicity observed in the study. Only trace amounts of this compound however were found in the authors extract. Specifically, 0.2  $\mu$ g per 100  $\mu$ l CgSE was detected in the crude extract. Therefore, the calculated effective concentration used in this study was 19.6 nM, significantly lower than its reported cytotoxic threshold (4  $\mu$ M) (Amiel et al., 2012). This quantity cannot account for the cytotoxic effects shown here, suggesting the presence of additional active compound(s). Interestingly, several additional cytotoxic compounds isolated by Amiel et al. (2012) may have played an important role in the observed cytotoxicity. For instance,  $\alpha$ -pinene and  $\alpha$ -terpineol have been demonstrated to exhibit high anti-proliferative activity in human erythroleukemia K562 cells (IC<sub>50</sub> = 117.3  $\mu$ M and 75.0  $\mu$ M, respectively) (Lampronti et al., 2006). In addition, Nerolidol, has been demonstrated to reduce the viability of Caco-2 cells (Vinholes et al., 2014) at high concentrations; Thus, it cannot be excluded that several factors cooperate in CgSE cytotoxic effects.

## 5. Conclusion

In conclusion, we have demonstrated that an ethanolic extract of Cg sap strongly induces apoptosis in immortalized and transformed human epidermal cell lines, but not in normal fibroblasts or in human skin explants. This effect targets cells at a post-replicative and pre-mitotic, or early mitotic stage. Therefore it is selective for proliferating cells, and may be of therapeutic value for the treatment of homeostatic disorders. Further work is required to identify the compounds involved and to evaluate their therapeutic potential.

## Conflict of interest

The authors declare no conflict of interest.

## Acknowledgements

We would like to dedicate this article to the memory of Professor Yoram Milner, who has passed away before this study was achieved. We are immeasurably indebted to him, professionally and personally. The study was supported by grants from the ICA Foundation and the Ministry of Science, Technology and Space.

## References

- Abdul-Ghani, A.S., Amin, R., 1997. Effect of aqueous extract of *Commiphora opobalsamum* on blood pressure and heart rate in rats. *J. Ethnopharmacol.* 57, 219–222.
- Agrawal, H., Kaul, N., Paradkar, A.R., Mahadik, K.R., 2004. HPTLC method for guggulsterone. I. Quantitative determination of E- and Z-guggulsterone in herbal extract and pharmaceutical dosage form. *J. Pharm. Biomed. Anal.* 36, 33–41.
- Al-Howiriny, T.A., Al-Sohaibani, M.O., Al-Said, M.S., Al-Yahya, M.A., El-Tahir, K.H., Rafatullah, S., 2004a. Hepatoprotective properties of *Commiphora opobalsamum* ("Balessan"), a traditional medicinal plant of Saudi Arabia. *Drugs Under Exp. Clin. Res.* 30, 213–220.
- Al-Howiriny, T.A., Al-Yahya, M.A., Al-Said, M.S., El-Tahir, K.E.H., Rafatullah, S., 2004b. Studies on the pharmacological activities of an ethanolic extract of Balsean, *Commiphora opobalsamum*. *Pak. J. Biol. Sci.* 7, 1933–1936.
- Al-sieni, A.I., 2014. The antibacterial activity of traditionally used *Salvadora persica* L. (miswak) and *Commiphora gileadensis* (palsam) in Saudi Arabia. *Afr. J. Tradit. Complement. Altern. Med.: AJTCAM/Afri. Netw. Ethnomed.* 11, 23–27.
- Amiel, E., Ofir, R., Dudai, N., Soloway, E., Rabinsky, T., Rachmilevitch, S., 2012.  $\beta$ -Caryophyllene, a compound isolated from the Biblical Balm of Gilead (*Commiphora gileadensis*). Is a selective apoptosis inducer for tumor cell lines. *Evid.-Based Complement. Altern. Med.: eCAM* 2012, 872394.
- Caillat, C., Perrakis, A., 2012. Cdt1 and geminin in DNA replication initiation. *Subcell. Biochem.* 62, 71–87.
- Chan, K.S., Koh, C.G., Li, H.Y., 2012. Mitosis-targeted anti-cancer therapies: where they stand. *Cell Death Dis.* 3, e411.
- Gandarillas, A., Freije, A., 2014. Cycling up the epidermis: reconciling 100 years of debate. *Exp. Dermatol.* 23, 87–91.
- Hanahan, D., Weinberg, R.A., 2011. Hallmarks of cancer: the next generation. *Cell* 144, 646–674.
- Hepper, N.F., Taylor, J.E., 2004. Date palms and opobalsam in the Madaba Mosaic map. *Palestine Explor. Q.* 136, 35–44.
- Hong, C.E., Lyu, S.Y., 2011. Anti-inflammatory and anti-oxidative effects of Korean red ginseng extract in human keratinocytes. *Immune Netw.* 11, 42–49.
- Iluz, D., Hoffman, M., Gilboa-Garber, N., Amar, Z., 2010. Medicinal properties of *Commiphora gileadensis*. *Afr. J. Pharm. Pharmacol.* 4, 516–520.
- Jones, K.H., Senft, J.A., 1985. An improved method to determine cell viability by simultaneous staining with fluorescein diacetate-propidium iodide. *J. Histochem. Cytochem.* 33, 77–79.
- Kleszczynski, K., Ernst, I.M., Wagner, A.E., Kruse, N., Zillikens, D., Rimbach, G., et al., 2013. Sulforaphane and phenylethyl isothiocyanate protect human skin against UVR-induced oxidative stress and apoptosis: role of Nrf2-dependent gene expression and antioxidant enzymes. *Pharmacol. Res.* 78, 28–40.
- Lampronti, I., Saab, A.M., Gambari, R., 2006. Antiproliferative activity of essential oils derived from plants belonging to the Magnoliophyta division. *Int. J. Oncol.* 29, 989–995.
- Orth, J.D., Tang, Y., Shi, J., Loy, C.T., Amendt, C., Wilm, C., et al., 2008. Quantitative live imaging of cancer and normal cells treated with kinesin-5 inhibitors indicates significant differences in phenotypic responses and cell fate. *Mol. Cancer Ther.* 7, 3480–3489.
- Pal, H.C., Sharma, S., Elmets, C.A., Athar, M., Afaq, F., 2013. Fisetin inhibits growth, induces G(2)/M arrest and apoptosis of human epidermoid carcinoma A431 cells: role of mitochondrial membrane potential disruption and consequent caspases activation. *Exp. Dermatol.* 22, 470–475.
- Portugal-Cohen, M., Soroka, Y., Ma'or, Z., Oron, M., Zioni, T., Bregegere, F.M., et al., 2009. Protective effects of a cream containing Dead Sea minerals against UVB-induced stress in human skin. *Exp. Dermatol.* 18, 781–788.
- Portugal-Cohen, M., Soroka, Y., Frusic-Zlotkin, M., Verkhovskiy, L., Bregegere, F.M., Neuman, R., et al., 2011. Skin organ culture as a model to study oxidative stress, inflammation and structural alterations associated with UVB-induced photodamage. *Exp. Dermatol.* 20, 749–755.
- Sakaue-Sawano, A., Kurokawa, H., Morimura, T., Hanyu, A., Hama, H., Osawa, H., et al., 2008. Visualizing spatiotemporal dynamics of multicellular cell-cycle progression. *Cell* 132, 487–498.
- Shen, T., Wan, W., Yuan, H., Kong, F., Guo, H., Fan, P., et al., 2007. Secondary metabolites from *Commiphora opobalsamum* and their antiproliferative effect on human prostate cancer cells. *Phytochemistry* 68, 1331–1337.
- Shen, T., Yuan, H.Q., Wan, W.Z., Wang, X.L., Wang, X.N., Ji, M., et al., 2008. Cycloartane-type triterpenoids from the resinous exudates of *Commiphora opobalsamum*. *J. Nat. Prod.* 71, 81–86.
- Shen, T., Li, G.H., Wang, X.N., Lou, H.X., 2012. The genus *Commiphora*: a review of its traditional uses, phytochemistry and pharmacology. *J. Ethnopharmacol.* 142, 319–330.

- Shen, F., Qi, J., Xu, F., Ning, L., Pang, R., Zhou, X., et al., 2013. Age-related distributions of nine fasting plasma free fatty acids in a population of Chinese adults. *Clin. Chim. Acta* 415, 81–87.
- Shishodia, S., Sethi, G., Ahn, K.S., Aggarwal, B.B., 2007. Guggulsterone inhibits tumor cell proliferation, induces S-phase arrest, and promotes apoptosis through activation of c-Jun N-terminal kinase, suppression of Akt pathway, and downregulation of antiapoptotic gene products. *Biochem. Pharmacol.* 74, 118–130.
- Vinholes, J., Goncalves, P., Martel, F., Coimbra, M.A., Rocha, S.M., 2014. Assessment of the antioxidant and antiproliferative effects of sesquiterpenic compounds in in vitro Caco-2 cell models. *Food Chem.* 156, 204–211.
- Wang, Z., Sun, Y., 2010. Targeting p53 for novel anticancer therapy. *Transl. Oncol.* 3, 1–12.